Influence of the Built-in Voltage on the Fill Factor of Dye-Sensitized Solar Cells

G. Kron, U. Rau,* and J. H. Werner

Institute of Physical Electronics (ipe), University of Stuttgart, Pfaffenwaldring 47, 70569 Stuttgart, Germany

Received: July 14, 2003; In Final Form: October 16, 2003

Dye-sensitized solar cells with different front contact materials to the nanoporous TiO_2 layer are used to investigate the influence of the front contact barrier on the photovoltaic performance. The study uses devices that have SnO_2:F, ZnO:Al, Al, or Au contacts underneath an amorphous TiO_2 blocking layer and the nanocrystalline TiO_2. These devices are illuminated via the semitransparent platinum back contact. Variations of the front contact have no significant influence on the open circuit voltage of the devices. In contrast, the fill factors of the solar cells exhibit systematic differences. The experimental current/voltage curves are fitted to a simple model that uses two diodes, one corresponding to the front contact/TiO_2 interface and a second one for the TiO_2/electrolyte interface.

Introduction

Dye-sensitized solar cells (DSSC)[1] are an interesting low-cost alternative to conventional solar cells and therefore have attracted considerable interest during the past decade. The basic photovoltaic action of these devices has been studied extensively in the past. After photoexcitation of the dye[2] and ultrafast injection of the excited electrons into the conduction band of the TiO_2,[3,4] the charge carrier transport occurs by diffusion[5,6] in the nanoporous TiO_2 network toward the contacting material.[7,8] According to basic, theroretical considerations,[9,10] numerical modeling,[8,11] and experimental data,[12] an (equilibrium) built-in voltage V_b^0 evolves close to the interface between the nanoporous TiO_2 and the contacting SnO_2:F front electrode. However, the importance of this junction potential V_b^0 for the photovoltaic performance of the DSSC is still controversially discussed.[9,10,13−15]

Schwarzburg and Willig[9] postulate a key role of the built-in voltage V_b^0 for charge separation and, in consequence, for the photovoltaic action in the DSSC. The origin of V_b^0 lies in the difference between the work function E_W of the substrate material and the redox potential E_{redox} of the electrolyte. The built-in voltage is caused by the negatively charged ions in the electrolyte surrounding the nanoporous TiO_2 close to its contact. Dependent on the size of the TiO_2 nanoparticles, the field region extends only 10−20 nm into the TiO_2 network. Schwarzburg and Willig[9] gave an estimate for the magnitude of the built-in voltage $V_b^0 \approx 0.7$ eV.[9] Thus, the magnitude of the built-in voltage is roughly sufficient to accommodate the external voltage V with the built-in voltage $V_b = V_b^0 - V \geq 0$ at a bias voltage V corresponding to the open circuit voltage V_{OC} that is typically $V_{OC} \approx 0.7$ V for DSSC. According to Schwarzburg and Willig[9] the equilibrium value V_b^0 sets an upper limit for the achievable V_{OC}.

Another group of publications[10,13,14] discards the importance of V_b^0 for the photovoltaic action of the DSSC. Within the arguments of refs 10, 13, 14, and 15, there is no limitation for the open circuit voltage due to the value of V_b^0. Note that V_{OC} of a typical DSSC is approximately 0.7 V at room temperature and hence is significantly larger than the estimate $V_b^0 \approx 0.3$ of Cahen and co-workers.[10] The fundamental upper limit for V_{OC} within the arguments of Ref 10 is given by the difference between the TiO_2 conduction band energy $E_C^{TiO_2}$ and the redox energy E_{redox} of the electrolyte.

Important experiments on possible limitations of the photovoltaic performance of DSSC by different front contact materials and, therefore, by variations in the built-in voltage were recently reported by Pichot and Gregg.[14] These authors used a series of DSSCs with a variety of front contact materials covering a range of work functions of 1.4 eV and demonstrated that these devices exhibit no significant difference in V_{OC}. With these experiments, Pichot and Gregg[14] established that V_{OC} is not affected by the front contact arrangement but is instead determined by the generation/recombination kinetics of the TiO_2/electrolyte/dye system. However, the experiments in ref 14 did not make use of the complete set of photovoltaic parameters, i.e., V_{OC}, short circut current density J_{SC}, and fill factor FF.

The idea of the present paper is to use complete DSSCs having different front contact materials and to investigate the influence of these contact variations on all photovoltaic parameters, i.e., on the complete illuminated current density (J)/voltage (V) characteristics of the devices. By these means, we hope to add more complete arguments to the ongoing debate that cumulates in a rather fundamental question: Is there a requirement for a charge-separating field in a photovoltaic device? The answer given in the present paper is "no" , concerning the buildup of a photovoltage. The answer, however, is "yes" , if one asks for a device that is well performing under operation conditions, i.e., which possesses not only V_{OC} and J_{SC} but also a reasonable fill factor FF.

Experiment

For the preparation of the DSSCs under investigation, we use glass substrates covered with four different conducting materials: the standard SnO_2:F with work function $E_w(SnO_2) \approx 4.8$ eV,[16] Al with $E_w(Al) \approx 4.3$ eV,[17] Au with $E_w(Au) \approx 5.1$ eV,[17] and ZnO:Al. Since ZnO sputtered under standard conditions is not stable for temperatures $T > 400$ °C, i.e., for temperatures necessary during the cell preparation process, we use a more stable ZnO sputtered at $T \approx 450$ °C. The work

* Corresponding author. Telephone: +49 711 6857199. Fax: +49 711 6857143. E-mail: uwe.rau@ipe.uni-stuttgart.de.

10.1021/jp036039i CCC: $25.00
Published on Web 11/07/2003

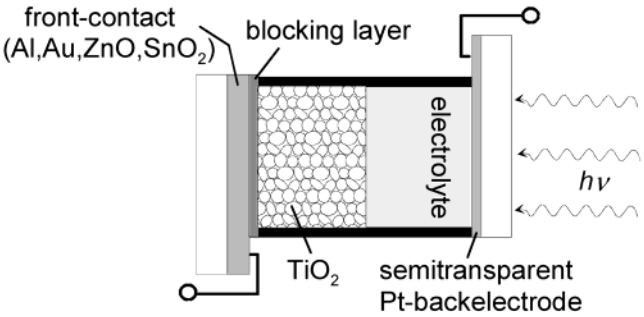

Figure 1. Sketch of the DSSC under investigation. The solar cells are illuminated through the semitransparent Pt back-electrode.

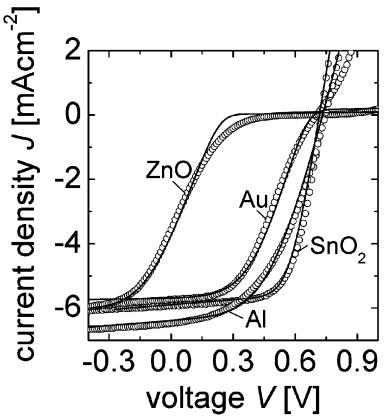

Figure 2. Experimentally measured *J*/*V* characteristics of the four devices under investigation (open circles). The influence on the fill factor for the DSSCs with higher work functions (Au and ZnO) can clearly be seen. The experimental data are fitted to the experimental circuit shown in Figure 1b (solid lines). The good match between theory and experiment allows us to determine the values for the barrier height Φ_b from the fits (cf. Table 1).

function of these ZnO:Al layers is determined relative to that of SnO_2:F by ultraviolet photoelectron spectroscopy (UPS) measurements with the result that $E_w(\text{ZnO:Al}) \approx E_w(SnO_2) - 0.2$ eV.

In view of the fact that we are dealing with a reactive contact formation, we do not expect that the differences of the work functions would lead to proportional changes in the barrier heights as predicted by the Mott−Schottky rule $\Phi_b = E_w - \chi_{TiO_2}$. However, the choice of different materials should enable to find unambiguous trends like in the earlier work of Pichot and Gregg.[14]

The device structures are shown in Figure 1 featuring the important detail that the different front contact materials are covered by a sprayed TiO_2 blocking layer prior to screen printing the nanocrystalline TiO_2 paste. By use of a blocking layer with a thickness of about 80 nm, parasitic redox reactions of the electrolyte at the front contact material are suppressed. Other details for the preparation of our DSSC were given elsewhere.[18] To enable illumination of the photovoltaic active part of the devices also with the nontransparent Al or Au front electrodes, we use semitransparent Pt back-electrodes with a thickness d_{Pt} of approximately 5 nm. As shown in Figure 1, illumination of all samples occurs through the Pt back-contact.

Results

Figure 2 shows the experimental *J*/*V* characteristics of the DSSCs (under illumination, open circles) with the four different contact materials: Al, SnO_2, ZnO, and Au. Since the semitransparent Pt back-electrode partly absorbs the incoming photons, the values of all short circuit current densities $J_{sc} \approx 6$ mAcm^{-2} are relatively low. Whereas the standard SnO_2:F contact yields the best efficiency, mainly because of the high fill-factor, the front contact materials with higher E_w and therefore lower V_{bi}^0, i.e., ZnO and Au, lead to degenerate, S-shaped *J*/*V* characteristics. The *J*/*V* characteristic of Al-front contact (lowest E_w) exhibits a relatively low-fill factor though there is no indication for an influence from a front contact barrier similar to the characteristic shape obtained from the Au and ZnO devices. In fact, the reason for the low fill factor of the Al device is instead due to the high series resistance R_s that most likely results from an oxide layer which forms during the preparation of the TiO_2 film at $T \approx 450$ °C.

TABLE 1: Summary of the Solar Cell Parameters Open Circuit Voltage V_{OC}, Series and Parallel Resistance R_S and R_P, Barrier Height Φ_b, and Equilibrium Built-in Voltage V_{bi}^0 Corresponding to the Four Devices with the Four Front Contact Materials with Different Work Functions E_W

contact material	E_W (eV)	V_{OC} (V)	Φ_b (eV)	R_S (Ω cm^2)	R_P (kΩ cm^2)	V_{bi}^0 (V)
SnO_2:F	4.8	0.72	≤0.6	14	50	≥0.6
Al	4.3	0.75	≤0.5	30	50	≥0.7
ZnO:Al	5.0	0.66	1.1	30	10	0.1
Au	5.1	0.70	0.7	18	10	0.5

The values of V_{oc} differ only slightly (but consistently with E_w). While $V_{oc} = 0.75$ V of the Al-DSSC lies above $V_{oc} = 0.72$ V of the standard device, we find $V_{oc} = 0.7$ V (Au) and $V_{oc} = 0.66$ V (ZnO) of the DSSCs with the higher work functions (see also Table 1). The maximum difference ΔV_{oc} of the open circuit voltage $\Delta V_{oc} = 0.09$ V is, however, small compared to the difference in work functions $\Delta E_w = 0.8$ eV. Note that similar small deviations in V_{oc} were reported earlier by Pichot and Gregg.[14] We are, therefore, up to this point consistent with these earlier results. However, the analysis of the present *J*/*V* characteristics uncovers large variations of the fill factors with characteristic S-shaped degradation behavior in the case of Au- and ZnO-contact devices. The simple contact barrier model outlined in the next section will provide an explanation for this type of degradation.

Model

Following the ideas outlined earlier,[19] we treat the DSSC as a series connection of a Schottky diode with barrier height Φ_b, representing the SnO_2:F/TiO_2 interface, and the main diode, which corresponds to the electron injection from the TiO_2 into the electrolyte. Let us assume that the current density *J* through the field region of the junction is dominated by thermionic emission of electrons from the TiO_2 into the SnO_2:F or into another contact material according to[20]

$$J = A^* T^2 \exp\left(\frac{-\Phi_b}{kT}\right)\left[1 - \exp\left(\frac{qV_l}{kT}\right)\right] \quad (1)$$

with A^* being the effective Richardson constant of TiO_2, *q* the elementary charge, *T* the absolute temperature, *k* the Boltzmann constant and V_l is the loss voltage that drops over the front contact as shown in Figure 3a. Since current continuity holds through the complete device, the current density *J* as given in eq 1 has also to fulfill the current−voltage relationship of the main diode, i.e.

$$J = J_0\left[\exp\left(\frac{qV_{int}}{nkT}\right) - 1\right] - J_{SC} \quad (2)$$

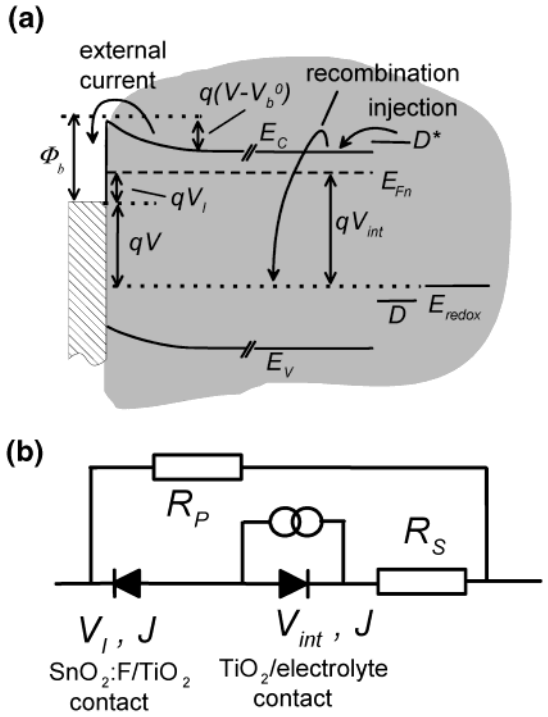

Figure 3. (a) Effective band diagram of the DSSC under illumination considering a situation where the internal photovoltage V_l exceeds the zero-bias built-in voltage V_b^0. Here, a barrier $V - V_b^0$ builds up at the front contact/TiO_2 interface such that under working conditions of the solar cell a loss voltage V_l might diminish the external voltage V available at the contacts. (b) Equivalent circuit of the DSSC: A series connection of a Schottky diode for the front contact/TiO_2 interface and of the main, photovoltaic active, diode together with two resistors for the series resistance R_S and the parallel resistance R_P.

In eq 2, J_0 denotes the saturation current density and n the ideality factor of the main diode. For a given current density J, the voltages V_l and V_{int} are calculated from eqs 1 and 2, respectively and $V = V_{int} - V_l$ finally yields the J/V characteristics of the equivalent circuit shown in Figure 3b in the range

$$A^*T^2 \exp\left(\frac{-\Phi_b}{kT}\right) > J > -J_{SC} - J_0 \qquad (3)$$

It is important to note that, in the equivalent circuit of Figure 3b, V_{int} and V_l denote the voltage drops over two distinct diodes. Contrarily, in the band diagram of Figure 3a, V_{int} and V_l do not show up as measurable electrostatic quantities; instead, $V_{int} = (E_{Fn}^{TiO_2} - E_{redox})/q$ is defined as the difference between the electron quasi-Fermi level $E_{Fn}^{TiO_2}$ in the TiO_2 and the redox energy E_{redox} of the electrolyte and $V_l = (E_{Fn}^{TiO_2} - E_{Fn}^{cont})/q$ is the difference between $E_{Fn}^{TiO_2}$ and the Fermi energy E_{Fn}^{cont} in the contact. Hence, V_{int} and V_l are only formal voltages that respectively determine the recombination or the collection kinetics of charge carriers. Only the external voltage $V = V_{int} - V_l$ corresponds to an electrostatic potential drop that is actually built up by electrostatic charge changes in the junction.

In the case of a small or zero (dark) built-in voltage V_b^0, under operating conditions we get a remaining potential $V_b = V_b^0 - V$ that is negative as sketched in Figure 3a. In such a situation, photoelectrons from the TiO_2 have to overcome a significant potential barrier between the TiO_2 and the SnO_2:F or another contact material. The question whether photoelectrons contribute to the photocurrent is a matter of the collection probability vs the recombination probability under the given bias condition. This probability ratio, however, corresponds to the current continuity condition obtained by equalizing eqs 1 and 2.

Under open circuit conditions, no electrons have to be driven over the potential barrier and, therefore, Φ_b does not affect the open circuit voltage V_{OC} and is exclusively determined by the difference $E_{Fn}^{TiO_2} - E_{redox}$, i.e., $V_{OC} = V_{int}$. Contrarily, the potential barrier, indicated in Figure 3a, leads to resistive losses under working conditions, since electrons have to overcome the barrier. Even in the best case, namely electronic transport by thermionic emission as expressed by eq 1, we have to envision a finite loss voltage V_l that subtracts from the internal voltage V_{int} and therefore degrades the fill factor FF of the J/V characteristic for barrier heights $\Phi_b > 0.6$ eV.[19] Considering the relationship $\Phi_b + qV = E_c - E_{redox} + q(V - V_b^0)$ from Figure 3a, we find the relationship

$$\Phi_b + qV_b^0 = E_c - E_{redox} \qquad (4)$$

We note that models for secondary diodes in solar cells similar to that outlined above are regularly used, e.g. for CdS/Cu(In,Ga)Se_2[21] or a-Si:H/c-Si[22] heterojunctions to explain fill factor degradations that, in these devices, are often encountered at T considerably below room temperature. We notice further that the above simple version of a double diode model is not suitable to model the dark forward current of the DSSC because the, then reverse biased, Schottky diode would block the current through the whole device as soon as $V > V_b^0$. For this situation a more leaky reverse characteristics of the secondary diode by tunneling[23] or by barrier inhomogeneities[24] would allow the injection of electrons from the front contact into the conduction band of the TiO_2. In fact, the anticipated high electrical fields at the TiO_2/front contact interface[8,9,14] would allow for a less pronounced blocking behavior at this interface. A corresponding refinement of the present model would however not change our main conclusions that will be discussed in the following.

Discussion

Figure 2 compares the experimental J/V characteristics of all four devices (symbols) with the fits (solid lines) to our model. To improve the fitting result, we have also included the series and parallel resistance R_s and R_p as summarized in Table 1. From the fitting procedure, we obtain the barrier heights Φ_b that correspond to the four different front contact materials and their interface to the TiO_2. In the case of the SnO_2 and the Al, we can only give an upper limit for Φ_b, i.e., $\Phi_b \leq 0.6$ eV for SnO_2 and $\Phi_b \leq 0.5$ eV for the Al. This is because at room temperature the voltage drop V_l resulting from such small Φ_b is too small to be detected. However, the barrier heights for the Au and the ZnO contacts with $\Phi_b = 0.7$ eV (Au) and $\Phi_b = 1.1$ eV (ZnO) significantly modify the J/V characteristics and are, therefore, determined by the fitting procedure. The barrier heights for the high-work function materials is considerably higher than those of the SnO_2 or the Al device. The minimum span of Φ_b within our experiments is therefore 0.6 eV and, thus, considerably larger than the differences of V_{OC} among the different devices. We note that the extracted barrier heights Φ_b are compatible with the sequence of work functions E_W of the different contact materials. We do however not find a proportionality between the measured barrier heights and E_W as expected for Schottky contacts made metals having different work functions.[25] This is partly because of the fact that we are dealing with a highly nonideal system involving a highly reactive environment during contact formation and also because our fitting procedure analyzes the contact only as the second diode in the system. We estimate therefore the accuracy of our results to only ± 0.1 eV. Thus, the present setup and the model

might be not the best choice for the determination of Schottky barrier heights, it is, however, successful in explaining the consequences of contact barriers on the photovoltaic performance of DSSCs.

Finally, we use eq 4 for estimating the built-in voltages in the different DSSCs. The difference $E_c - E_{redox}$, was determined in Ref 19 from the temperature dependence of V_{OC} as $E_c - E_{redox} \approx 1.2$ eV. With this value, the built-in voltages are given by $V_b^0 \geq 0.7$ eV for the Al, $V_b^0 \geq 0.6$ eV for the SnO_2, $V_b^0 = 0.5$ eV for the Au, and $V_b^0 = 0.1$ eV for the ZnO device, respectively (see also Table 1). Thus, the measured values of V_{OC} exceed in all cases the estimates of V_b^0 or at least the lower limits. Note that a certain allowance for $V_{OC} - V_b^0 > 0$ was already demonstrated by the numerical simulations of Ferber and Luther[11] and is also discussed in ref 26. However, $V_{OC} - V_b^0 > 0$, at least from a theoretical point of view,[27] is not a privilege of DSSCs or other organic solar cells. Nevertheless, in all solar cells the transport problems arising from $V_{OC} - V_b^0 > 0$ cost a prize in terms of losses of the output power[28] as in the case of the present Au and ZnO devices with their considerable degradation of the fill factor. Note that, e.g., $V_b^0 = 0.5$ eV for the Au device is larger than the value of $V_b^0 = 0.3$ eV estimated in ref 10 for the standard DSSC. However, our above results suggest that $V_b^0 = 0.5$ eV already impedes a well-behaved photovoltaic device, and our lower limit $V_b^0 \geq 0.6$ eV for the standard (SnO_2) devices is relatively close to the estimate of ref 9.

Conclusions

Experiments with variations of the front contact material to the TiO_2 network of DSSC show that the resulting variations of the built-in voltage have no large effect (if any) on the open circuit voltage V_{OC} of those devices. Thus, V_{OC} is rather determined by the steady state between photocarrier generation and recombination in the TiO_2/dye/electrolyte system.[10,13,14] A limitation of V_{OC} in DSSCs by the built-in voltage V_b^0 does not occur because these devices simply have no (significant) recombination path that is directly correlated to the built-in voltage such as, e.g., interface recombination in solid-state heterojunctions.[29]

Nevertheless, the imperative of a dark built-in voltage in DSSC (and in solar cells in general) is enforced by the requirement *for charge separation under working conditions.* As shown congruently by our experiments and modeling, an insufficient built-in voltage will first of all lead to fill factor degradations. This undesirable loss of photovoltaic performance is a result of rather fundamental transport restrictions such as, in the present situation, thermionic emission between the photovoltaic absorber and the contact material. By definition, such restrictions are irrelevant under *open circuit conditions*, i.e., in the absence of electronic transport. However, when considering a solar cell *under operating conditions*, there is hardly a possibility to deny the general importance of a dark built-in voltage.

Acknowledgment. The authors gratefully acknowledge the support by Sony International (Europe). We thank K. Taretto, G. Nelles, M. Duerr, T. Miteva, and A. Yasuda for collaboration and discussion. We also thank C. Heske from the University of Würzburg for the UPS measurement of the ZnO substrates.

References and Notes

(1) O'Regan, B.; Grätzel, M. *Nature (London)* **1991**, *353*, 737−740.
(2) Grätzel, M. *Comments Inorg. Chem.* **1991**, *12*, 93−111.
(3) Tachibana, Y.; Moser, J. E.; Grätzel, M.; Klug, D. R.; Durrant, J. *J. Phys. Chem. B* **1996**, *100*, 20056−20062.
(4) Cherepy, N. J.; Smestad, G. P.; Grätzel, M.; Zhang, J. Z. *J. Phys. Chem. B* **1997**, *101*, 9342−9351.
(5) Solbrand, A.; Lindström, H.; Rensmo, H.; Hagfeldt, A.; Lindquist, S. E.; Södergren, S. *J. Phys. Chem. B* **1997**, *101*, 2514−2518.
(6) Cao, F.; Oskam, G.; Meyer, G. J.; Searson, P. C. *J. Phys. Chem. B* **1996**, *100*, 17021−17027.
(7) O'Regan, B.; Moser, J.; Anderson, M.; Grätzel, M. *J. Phys. Chem.* **1990**, *94*, 8720−9726.
(8) Bisquert, J.; Garcia-Belmonte, G.; Fabregat-Santiago, F. *J. Solid-State Electrochem.* **1999**, *3*, 337−347.
(9) Schwarzburg, K.; Willig, F. *J. Phys. Chem. B* **1999**, *103*, 5743−5746.
(10) Cahen, D.; Hodes, G.; Grätzel, M.; Guillemoles, J. F.; Riess, I. *J. Phys. Chem. B* **2000**, *104*, 2053−2059.
(11) Ferber, J.; Luther, J. *J. Phys. Chem. B* **2001**, *105*, 4895−4903.
(12) Levy, B.; Liu, W.; Gilbert, S. E. *J. Phys. Chem. B* **1997**, *101*, 1810−1816.
(13) Huang, S. Y.; Schlichthörl, G.; Nozik, A. J.; Grätzel, M.; Frank, A. J. *J. Phys. Chem. B* **1997**, *101*, 2576−2582.
(14) Pichot, F.; Gregg, B. A. *J. Phys. Chem. B* **2000**, *104*, 6−10.
(15) Zaban, A.; Meier, A.; Gregg, B. A. *J. Phys. Chem. B* **1997**, *101*, 7985−7990.
(16) Grovenor, C. R. M. *Microelectronic Materials*; IOP Publishing: Bristol, England, 1989.
(17) Weast, R. C.; Astle, M. J. *CRC Handbook of Chemistry and Physics*; CRC Press: Boca Raton, FL, 1980.
(18) Kron, G.; Egerter, T.; Nelles, G.; Yasuda, A.; Werner, J. H.; Rau, U. *Thin Solid Films* **2002**, 403−404, 242−246.
(19) Kron, G.; Egerter, T.; Werner, J. H.; Rau, U. *J. Phys. Chem. B* **2003**, *107*, 3556−3564.
(20) Rhoderick, E. H.; Williams, R. H. *Metal-Semiconductor Contacts*, 2nd ed., Clarendon Press: Oxford, England, 1988; p 15.
(21) Eisgruber, I. L.; Granata, J. E.; Sites, J. R.; Hou, J.; Kessler, J. *Solar Energy Mater. Solar Cells* **1998**, *53*, 367−377.
(22) Jensen, N.; Rau, U.; Werner, J. H. *Mater. Res. Soc. Symp. Proc.* **2000**, *609*, A13.1.1−6.
(23) Padovani, F. A.; Stratton, R. *Solid-State Electron.* **1966**, *9*, 695−707.
(24) Werner, J. H.; Güttler; G. *J. Appl. Phys.* **1991**, *69*, 1522−1533.
(25) Cowley, A. M.; Sze, S. M. *J. Appl. Phys.* **1965**, *36*, 3212−3220.
(26) Gregg, B. A.; Hanna, M. C. *J. Appl. Phys.* **2003**, *93*, 3605−3613.
(27) Würfel, P. *Physica E* **2002**, *14*, 18−26.
(28) Rau, U.; Kron, G.; Werner, J. H. *J. Phys. Chem. B* **2003**, *107*, in press.
(29) Bube, R. H. *Photoelectronic Properties of Semiconductors*; Cambridge University Press: Cambridge, England, 1992; p 257.